Accepted Manuscript

Title: Charts based on millions of fluid dynamics simulations provide a simple tool to estimate how far from its source a specific blood stain can be found

Author: Daniel Attinger

Please cite this article as: Attinger D, Charts based on millions of fluid dynamics simulations provide a simple tool to estimate how far from its source a specific blood stain can be found, *Forensic Science International* (2019), https://doi.org/10.1016/j.forsciint.2019.02.052

This is a PDF file of an unedited manuscript that has been accepted for publication. As a service to our customers we are providing this early version of the manuscript. The manuscript will undergo copyediting, typesetting, and review of the resulting proof before it is published in its final form. Please note that during the production process errors may be discovered which could affect the content, and all legal disclaimers that apply to the journal pertain.

Charts based on millions of fluid dynamics simulations provide a simple tool to estimate how far from its source a specific blood stain can be found

Daniel Attinger

Iowa State University, Mechanical Engineering Department, Ames IA 50010, USA

Highlights

- A large dataset of more than five million of numerically calculated trajectories of blood drops is produced and mined to determine the maximum distance between a blood stain and the source of the blood.
- The numerical results are presented as a set of charts that can be directly useful for investigative work in bloodstain pattern analysis.
- Results are presented using variables that are directly and easily observed on the crime scene, such as the stain size and its ellipticity.
- The packaging of complex physics into a tool that is simple to use and that does not require any knowledge of fluid dynamics is analog to a pregnancy test.
- Comparisons with existing reports of experiments and a limited set of experiments are consistent with the results of the proposed theoretical model.

Abstract

The bloodstain pattern analyst sometimes has to judge if a given stain could originate from a specific location. A wide range of values of the maximum distance that a blood drop can travel have been reported from experiments, ranging from less than one meter to more than 10 meter. Here we formulate the problem in a fluid dynamics and data mining framework. The fluid dynamics is solved with Newton's classical equation of motion coupled with well-established models for the gravity and drag forces that bend the trajectories of drops. The parameters screened are the drop size, initial velocity and launch angle, as well as the height of a blood source and the ceiling height. Combining a wide range of values of those five parameter commended the performance of more than 5 million fluid dynamic simulations. Results of those simulations have been searched and mined for parameters directly measurable on a crime scene, such as the stain size and stain ellipticity. The results are presented in simple charts. Those charts are easy to use, and do not require any knowledge of fluid dynamics from the analyst.

Introduction

Recently, fundamental research in BPA has augmented the science base and offered new venues for the development of tools and methods. For instance, several recent studies have improved the knowledge base and tools related to the determination of the region of origin of a stain or a spatter. For instance, a

method to infer the fall height of a dripping drop was proposed [1] based on a fluid dynamics analysis of the occurrence and abundance of spines -which are pointy deformation at the periphery of a stain. Uncertainties related to fluid dynamic conditions on the determination of the impact angle from stain inspection have been investigated quantitatively [2]. The fate of a dripping drop was characterized as a function of the impact conditions, with respect to spreading on various target materials [3]. Quantitative measurements were made of the wicking, rotation and deformation of stains caused by fabrics [4]. New fluid dynamic models of the atomization of blood have been tested against backward [5] and forward [6] gunshot spatters. Medium to large datasets of blood spatters [7] [8] have been made available, in high resolution, to the scientific community for the purpose of testing methods and data. High Speed videos describing the multiple physical phenomena related to BPA were produced [9], and quantitative measurements thereof have estimated the initial velocities and drop sizes [10]. State of the art image processing methods [11] were described to measure the multiple stains (more than 40,000 in some gunshot spatters). Also, blood is a complex fluid with properties that are not yet fully known. Its properties have been further characterized in terms of storage life [12] and extensional viscosity [13]. Trajectory models accounting for the effect of drag and gravity on drops were formulated and calibrated [14, 15]. Many of the rationale for these research efforts can be justified by the multiple and natural connections between fluid dynamics and bloodstain pattern analysis [16]. That latter reference presents the fluid dynamics concepts relevant to BPA, with relevant examples, and might help BPA practitioners and researchers who are not already familiar with fluid dynamics, understand of the fluid dynamics in the present manuscript.

Despite the above acceleration of research, it is not clear to the author if any of the above efforts has resulted in novel methods currently used in the field. It certainly takes time to vet academic progresses and to package these into useable tools. It is a complex task to change an industry. For instance, airline pilots still communicate with control towers using low quality analog radio, despite more advanced digital systems like FANS [17], which have been under development since at least the 1990s. Those digital systems provide clear voice quality with written transcription. Importantly, new forensic methods must be robust, easy to use, offer a significant improvement over the state of the art, with other desirable requirements such as a known uncertainty and error.

Here we address a practical problem relevant to BPA with a set of charts that can be used without knowledge of the complex underlying physics. The fluid dynamics is indeed packaged in a large data set of millions of simulation results, the useful results of which are provided as simple charts. The practical problem is as follows. The bloodstain pattern analyst sometimes has to assess if a given blood stain could have originated from a given location at a crime scene. Thus arises the question of how far a blood drop can be found from its blood source.

This question has been addressed experimentally in several studies. The location of stains furthest away (horizontally) from a blood source has been measured in studies of gunshots, where various guns, ammunition, settings and blood source have been used. Examples of blood sources include calves heads [18], a human cadaver filled with blood [19], foams or sponges soaked in blood [20, 21], or cavities filled with blood [6]. Some experimental results of blood spatters were selected for comparison with theoretical and numerical studies, and the maximum experimental distances were 70cm [22] for backspatters and 4 meter for forward spatter [6]. An anonymous literature review in the 2007 newsletter of the International Association of Bloodstain Pattern Analyst [23] mentions 12 references for "distance that backspatter

travels". Depending on the study cited, the maximum distances given are between 30cm ($\cong$ 1 foot) and 6.5 feet ($\cong$ 198cm). It is important to mention that not every one of the work cited [24-29] was focused on the same single issue of how far on drop can travel. Some studies were focused on how far sub mm-stains would travel [30], while some other were focused on the presence or not of stains on the hand holding the gun [28]. At the 2018 IABPA conference, the presentation "Slugger Slaying Caught on Tape" by John Bockrath and Ray Lugo describe a beating in a Walmart department store [31]. The beating was recorded by the surveillance cameras in a unique and gruesome piece of data. The victim was on the floor and did not move; their head was destroyed by repeated assaults with a baseball bat, and the furthest stain was found 33 feet ($\cong$ 10.1 m) away from the region of origin of the spatter, which as far as we know is the largest reported distance to date.

Note that there is little standardization in the above studies with respect to the blood (human or animal), its hematocrit (known or unknown), its temperature (ambient or heated), its container and the height of the blood source over the floor. The present theoretical work solves the problem in a general manner, with clearly stated assumptions. Comparisons with experimental data are consistent with the theory. The rest of the manuscript is organized as follows: a brief presentation of the theoretical framework leads to the results and their discussions, followed by a thorough description of the methods used to obtain those results.

Theoretical question and framework

The theoretical question addressed in this manuscript is represented in Figure 1: "A blood source at height h over a horizontal floor, in a room with ceiling at height H, generates drops with a broad and realistic range of diameters, initial velocities and launch angles. How far from the blood source can the drops travel?

Note that the theoretical question above corresponds to a physical and deterministic problem. By deterministic we mean a problem proceeding forward in time, from well-known initial conditions. Questions asked to forensic investigators are never that simple, as those questions are rather reconstruction problems. Indeed, in a bloody crime or accident, little is known about velocities and drop sizes. The available evidence is one or several stains, or patterns thereof, on a given target surface. The investigator can measure their orientations, sizes and shapes. The question asked by the bloodstain pattern analyst is thus not the deterministic question above ("How far can a blood drop travel from its source?"), but the slightly different question: "Considering a stain, what is the ensemble of locations in space from which it could have originated?" This reconstruction question could be solved by proceeding backward in time from impact conditions inferred from stain inspection, but this study takes a different route, in solving millions of time-forward trajectories and then mining the data for the results of interests, as follows.

To answer the two above questions, we first design and perform numerical simulations to calculate a data set of drop trajectories, screening a wide range of initial velocities and drop sizes, of room dimensions and of height of the blood source. The range of parameters is presented in Table 1.

Each trajectory is calculated by numerical integration of Newton's second law for a drop moving through the air, proceeding forward in time until the drop either hits the ceiling, the floor, or breaks up in flight. The calculation of the drag force is based on published models based on published correlations based on experiments. The drag model considers that drops deform in flight, and the corresponding increase of drag. Information on stain ellipticity is estimated from the numerically calculated impact angle, and stain size is estimated from widely used spreading correlations. The resulting data set is relatively large, corresponding to more than five millions of different trajectories. Numerical sorting and search of the data set is then performed to produce charts of interest for forensic reconstruction. Those charts are presented in the results section, with clear instructions on how to use these and on the underlying hypotheses. Results of the theoretical simulations are finally compared with several experiments documented in the BPA literature, as well as a limited set of gunshot spatter experiments performed in the context of this work. Details of the simulations and methods are provided in a later, specific section.

Results and Discussion

In figure 2, the ceiling height is 2.75 m (~9 feet) and some red trajectories are seen to hit and stop and the ceiling. Note also the small and fast drops (cyan) that ultimately fall almost vertically to the floor (on the right): those drops descend at terminal velocity, and create round stains that have lost any directionality.

Numerical results

In this section, several numerical results of interest to practitioners are provided. Figure 3 describes the maximum distance that a stain on the floor can be found away from a blood source, as a function of the stain size and ellipticity. This maximum distance is larger than 7 meter, and is reached by stains with equivalent diameters in the 10-50mm range. The size of the stain is expressed by its equivalent diameter, $d_S = \sqrt{\frac{4A}{\pi}}$, which is approximately equal to $\sqrt{WL}$, as represented in Figure 1, right. Above, the symbols A, W and L stand for the area of the stain, and the width and length of an ellipse fitted to the stain, respectively. The shape of the stain is defined by the ellipticity of a best-fitted ellipse $\varepsilon = \frac{W}{L}$. Other variables illustrated in Figure 1 such as ceiling height, height of blood source, drop diameter and drop velocity are allowed to take any combination of values of Table 1. On the left of the plot, the accumulation of vertical contours describe the fact that stains with sub-mm size do not travel far from the source, which is consistent with experimental observations that the "mist' produced by backspatter does not travel further than a few feet [23]. Since no constraints were set on the height of the blood source, of the ceiling, nor on the initial velocity, it is possible that some results for specific values of ceiling height and source height are smaller than in Figure 3. Examples of specific cases are in figures Figure 4 to Figure 6.

It is also possible to screen the numerical results for more specific situations, to obtain even more precise answers. For instance, let us assume that the position of the blood source is known, from, e.g. wound evidence or concurring testimony. This limits the range of source heights, as shown with the model photographs in Figure 4. Heights corresponding to the three positions (lying on the floor, sitting or standing) are listed in Figure 4a, in an exclusive way, assuming a height range that only corresponds to on given position.

Curves in Figure 4a describe the maximum and minimum horizontal distances between a stain and its source, with respective hatched and continuous color lines, as a function of the position of the source and the ellipticity of the stain. For instance, if the blood is known to originate from a standing person, and the measured ellipticity of the stain is 0.7, the red curves provide the maximum and minimum horizontal distances as $r_{min} \cong 3m$; $r_{max} \cong 6m$. Interestingly, results of the model reported in Figure 4a show that the curves for the "standing" and "sitting" heights do not extend all the way to the left of the figure. This illustrates that stains with low ellipticity values are not compatible with an arbitrary source height. Indeed, a search on the entire data set indicates that the minimum predicted stain ellipticity corresponding to a respective source height of 40cm or 140cm is 0.31 or 0.61, respectively. Thus, the model would indicate that a stain with ellipticity of, e.g., 0.5 could not originate from a height of (or larger than) 140cm. Figure 4b explains how to use Figure 4 to discriminate among possible and impossible locations of the victim: locations E and A are impossible because their horizontal distance to the stain is larger than r_{max}; location C is impossible because its horizontal distance to the stain is smaller than r_{min}; location F and E are not aligned with the main direction of the stain, thus impossible; location D is aligned with the main direction and within the correct distance, but the presence of the splashing features (also called wave cast-off) indicate that the drop flew from the opposite side of the stain, the side of location B. Thus only location B is compatible with the stain of interest. Note that we assume a specific uncertainty on the main direction of the stain, as in [32], and this uncertainty is represented by the thickness of the wedge. This angular uncertainty depends on several factors such as the target material, the size of the stain, and the impact angle. On the one hand, a round stain typical of normal impact will have angular uncertainty of +/-180°, which is a whole cylindrical cake. On the other hand, an elongated stain with ellipticity of about 0.4 corresponding to a slanted impact angle of about 40° will have angular uncertainty of a few degrees, say +/-3°. A tentative quantification of the uncertainty on the direction of stains on cardstock is in [33]. Also, if the investigation deals with persons of widely different heights or figure than the model in Figure 4, in-situ measurements with a model of similar size as the person of interest are necessary.

The problem in Figure 1 can better be addressed by considering the additional information of the stain size. Results in that case are reported with two plots in Figure 5, one for the maximum and one for the minimum horizontal distance that a stain can be found from its blood source. In the specific case of a stain with equivalent diameter of 20mm and an ellipticity of 0.7, Figure 5 determines the minimum distance as larger than 3.3m, while Figure 4 determines the distance as larger than 3m – without using information on the stain size. Thus, the additional information on stain size can reduce the uncertainty on the location of the blood source in specific cases.

Figure 7 has no practical use but informs on several aspects of the fluid dynamics at hand. It plots the same maximum distance between stain and blood source as Figure 3, however as a function of the initial drop size and drop velocity. Figure 7 is not directly useful on a crime scene, because drop size and initial

velocities are unknown. While past literature has associated typical drop sizes and velocities to specific events such as beatings and gunshot, recent optical measurements in [10] have shown that the single same atomization mechanism, a gunshot by Laber et al. [9], would generate a wide range of drops sizes and initial velocities. Interestingly, the drops that travel the farthest are those with average size (d ∈ [2mm − 6mm] and average velocity (V ≅ 14m/s). Faster drops corresponds to the white region in Figure 7, where drag overcomes surface tension and the drop breaks up in flight. Smaller drops suffer from a disproportionally strong drag, with respect to their inertia, and do not travel much – less than 2 meter for drops smaller thank 500 micrometer. Larger drops can only be thrown at velocities below 10m/s, to avoid break-up in flight. This explains that larger drops cannot travel as far as those with average size. Charts like Figure 7 summarize millions of numerical simulations and allow to see through various aspects of the physics of the problem, in a different way than via experiments.

In interpreting the numerical results, it is important to keep in mind the assumptions underlying the calculations presented here.

a) The model considers deformation and breakup of drops during flight under the effect of drag forces [34].
b) Blood properties are same as those of swine blood at 22°C [16].
c) Effects of wind and indoor air currents on the trajectories is considered negligible. See [14] for estimates of those effects. Similarly, it is assumed that muzzle gases do not modify the drop trajectories in the case of gunshot spatters.
d) Each drop travels independently from any other. The 'bird formation flight' effect in [5] is thus neglected. Consideration of this drag reduction effect might increase the maximum distance between drop and source, especially for situations where the launch angle is within a narrow range – like jets in e.g., arterial gushing.
e) The stains of interest are those found on the horizontal floor. Results are not directly applicable to stains found on a vertical wall or on the ceiling.
f) The spreading of stains on the non-absorbing target of interest is similar to that characterized on smooth cardstock [3].
g) The stain ellipticity is a simple function of the impact angle, shown in Figure 1, for any fluid dynamic conditions.

Experimental results: While this study is essentially theoretical, a small set experiments were also performed. The blood source was a cavity filled with blood, similar to the one used described in [6], set at height 1.3m. The blood source was hit by a full metal jacket bullet shot with either a rifle or a handgun. No attempt was made to screen the muzzle gases, as the gun was held relatively far from the blood source, about 250 cm. The floor of the shooting range was covered with 5 strips of 36''-wide butcher paper, corresponding to a total width of about 4.55 m (180'') and a length in the direction of the bullet path of about 10 meter. The ceiling of the shooting range was measured as 260cm. The most remote stains were circled with pencil on the butcher papers, which have been preserved. The horizontal distance between the most remote blood stain and the blood source was recorded. Two experiments were made with the handgun, and one with the rifle. Bullets and guns are described in Table 2.

Temperature in the shooting range was 15°C and the hematocrit of the pig's blood used was 39%. Maximum distances measured were 3.92 m for the rifle and 5.45 meter for the handgun.

Note that those experiments on how far a blood drop travels were not as extensive as the independent reports of the same cited in the introduction, but were produced within a larger effort focused on creating a data base of freely-available high-resolution spatters [7]. Gunshot experiments are good candidates to produce stains at large distances from their source, because gunshots produce a wide range [10] of drop velocities and drop sizes, including drop sizes and velocities likely to travel maximum distances, as predicted in Figure 7.

Considering the data reported in the introduction as well as the above experiment, maximum distances reported experimentally between a blood stain and its source vary between 30cm and 10 meter. Figure 8 compares experimental data with the numerical results of this manuscript.

In four out of five studies, the maximum distances reported experimentally are smaller than the maximum distances predicted by our simulations. This trend to be expected because the numerical simulations correspond to every possible combination of drop size, velocity, launch angle, while any experiments will only produce a subset of those combinations – although gunshot backspatters have been shown to produce 40,000 stains [8]. The fact that experiments only produce a subset of velocities and drop sizes also explains the scatter of the experimental data. One reported experimental result is larger than the theoretical maximum, by about 2 meter. This is unexpected, and the author remembers addressing the issue in the questions following the oral presentation [31]. Possibly, one or several assumptions of the numerical simulations presented here need to be revisited. The speaker hinted at the fact that the stain was possibly not pure blood but rather brain matter. Indeed tissues such as brain matter behave differently than fluids, because they have internal structure that maintain their cohesion. They behave differently in the way fragments are created upon impact; also, flying chunks of brain matter deform less than blood drops and are less likely to break up because of drag forces. Technically, the experimental data of [31] violates assumption (b) presented above. There is certainly a lot more physics to uncover in the world of bloodstain patterns.

Methods

There is a wide body of engineering literature describing the trajectories of flying drops, in relation to e.g. inkjet printing [16], fuel injection [35] or raindrops [36]. Thus simulations such as those presented here do not present specific difficulties beyond the challenge of running 4 millions of these within a reasonable amount of time. The simulation equations and framework are described below.

The trajectories of flying drops are described with an equation of motion based on Newton's law:

$$m_d \frac{d\vec{V}}{dt} = m_d\vec{g} - \vec{F_D}. \tag{1}$$

Above, $m_d, t, V, \vec{g}, \vec{F_D}$ are the drop mass, time, drop velocity, gravity acceleration and drag force, respectively. It is assumed that the air is quiescent, and that the interactions between drops are negligible Lift forces are also neglected – those would matter if the drop spins and such information is unavailable at the time of reconstruction.

To calculate the equation of motion (1), it is necessary to estimate the drag caused by the air on the travelling droplet. The drag force is defined as in [16]

$$\overrightarrow{F_D} = \rho_a C_D \frac{A_d}{2} V \overrightarrow{V}, \tag{2}$$

where ρ_a, A_d, V and $\overrightarrow{V}$ are the air density, the cross-sectional area of the undeformed droplet ($A_d = \pi d^2/4$), the velocity magnitude and velocity vector of the droplet, respectively. The dimensionless parameter C_D is a drag coefficient for isolated spherical particle, modified to account for the particle deformation that occurs at intermediate Weber number. Indeed, when the Weber number becomes larger than one, the drop becomes oblate, with a ratio of the largest diameter to the smallest that can be as high as 2 [37]. At higher drag, the drop has been observed to break up in flight, and those trajectories are excluded from the simulation. The drag coefficient has been validated against a wide body of experimental studies reviewed and synthetized by Loth [37], and is expressed as.

$$C_D = C_{D,sphere} + \Delta C_D \cdot \left(C_{D,deformed} - C_{D,sphere} \right). \qquad 0 \le We_a \le 13,400 \le Re_a \le 7000 \tag{3}$$

In the above equation,

$$\Delta C_D = 3.8 \times 10^{-3}(We_a Re_a^{0.2}) + 3 \times 10^{-5}(We_a Re_a^{0.2})^2 + 9 \times 10^{-7}(We_a Re_a^{0.2})^3 \tag{4}$$

is an empirical fit provided in [37] and based on experiments with drops of various fluids in air by Reinhart [38]. The Reynolds and Weber numbers are based on air as the fluid, as per their subscript a. The other terms in equation (3) are also provided in [37]: $C_{D,sphere}$ is a drag coefficient for an isolated spherical particle by Clift el al. [39]

$$C_{D,sphere} = \left[\frac{24}{Re_a} \left(1 + 0.15 Re_a^{0.687} \right) \right] + \frac{0.42}{1 + 42500 / Re_a^{1.16}} \qquad 0.1 \le Re_a \le 2 \times 10^5; \tag{5}$$

and the drag coefficient at to the maximum deformation is an empirical relation by Clift et al. [39]

$$C_{D,deformed} = \frac{8}{3} + \left[\frac{24}{Re_a} \left(\frac{2 + 3\mu^*}{3 + 3\mu^*} \right) \right],$$

(6)

with μ^* the ratio of the dynamic viscosities of the blood and the air. Comparison between the drag coefficient used in this study and the one correlated on experiments by Vargas et al. [36] showed no significant difference in the trajectories.

Once the drop hits the ceiling or the floor, the angle between its velocity and the target surface is used to estimate the stain ellipticity according to the relation $\sin(\alpha) \cong \frac{W}{L} = \epsilon$, and produce plots such as Figure 3 and Figure 4. To produce charts such as Figure 5, a relation is needed to estimate drop spreading and the correlation between drop size and the size of the resulting stain. For oblique impact, Adam [40] has

shown that a correlation exist between normal impact velocity and drop spreading. This correlation can be expressed [41] in the way proposed by Bousfield and Scheller [40, 42],

$$\beta = W/D = a(Re_N^2 Oh)^b. \tag{7}$$

Above, β is the spread ratio expressing how much the drop spreads upon impact. It is the ratio of the stain width over the initial drop diameter. The coefficients are specific to the impact surface, and here we use coefficients a=0.257 and b=0.235 [3], measured on smooth cardstock. Those correspond to a non-absorbing surface with average spreading, in the sense that drops would spread more on glass and less on plastic [3]. The Reynolds number $Re_N = \rho V_n d/\mu$ measures the ratio of the blood inertia normal to the impact surface to the viscous forces inside the drop, and the Ohnesorge number $Oh = \frac{\mu}{\sqrt{\rho d \sigma}}$ scales inertial with respect to the resisting viscous and surface tension forces. Symbols ρ, μ and σ, are the density, viscosity, and surface tension of the blood drop, respectively, and u is the velocity component normal to the target. The following values are used for the physical properties of air and blood: blood density $\rho = 1060$ kg/m³; surface tension between blood and air $\sigma = 59$ mN/m; dynamic viscosity of blood $\mu = 42$cP; dynamic viscosity of air $\mu_a = 1.98$ x10-5 Pa·s; density of the air $\rho_a = 1.229$ kg/m3. The blood properties correspond to swine blood, considered an adequate substitute for human blood in BPA experiments, at temperature of 22°C and hematocrit of 45% [3]. The critical Weber number for drop breakup in flight is set to 13, consistently with extensive experimental studies by Hsiang and Faeth [43].

The total number of simulations is the product of the numbers of each parameters in Table 1, p=9x21x28x27x35 simulations, which represents more than 5 million simulations. Simulations were conducted using the scientific computing language MATLAB [44] version 2013b, which is reasonably fast at integrating ordinary differential equations and excellent at manipulating large amounts of numerical data. Simulations took about 48 hours on a 2016 workstation (Intel i7 CPU at 2.7GHz, with 32GB of RAM). Results and input parameters of the simulations have been saved into a structured data file of about 28 GB. The resolution of the saved trajectories is 20cm or better, in terms of horizontal distance. The fate of the drop, which either hit the ceiling, hit the floor, or broke up in flight, is also saved in the data set. Sorts and search operations with were then used to identify the data required for the various plots of interest to BPA analysts.

Conclusion

A large dataset of more than four million of numerically calculated trajectories of blood drops is produced and mined to determine the maximum distance between a blood stain and the source of the blood. The governing equations are presented, and the results depend on the following variables: drop size, drop initial velocity and launch angle, height of blood source and height of ceiling. The numerical results are presented as a set of charts that can be directly useful for investigative work in bloodstain pattern analysis. Results are presented using variables that are directly and easily observed on the crime scene, such as the stain size and its ellipticity. The packaging of complex physics into a tool that is simple to use and that does not require any knowledge of fluid dynamics is analog to a pregnancy test. Throw-away pregnancy tests packages complex chemistry and biology, even fluid dynamics, in a way that is easy to use and produce reliable results. As such, the "pregnancy test" approach presented in this work is worthy

of pursuing to design tools for the BPA analyst, besides the classical approach which consists in teaching fluid dynamics to bloodstain pattern analysts. We would certainly recommend considering both approaches, considering that typical mechanical engineering programs at e.g., Iowa State University or EPFL allocate between 300 and 700 contact hours to teach fluid dynamics and the pre-required math and physics background to their undergraduate students. Comparisons with existing reports of experiments and a limited set of experiments are consistent with the results of the proposed theoretical model. The wide range of reported experimental values for the maximum travel distance of a blood drop warrants however further comparisons.

B[1]   L. Hulse-Smith, N. Z. Mehdizadeh, and S. Chandra, "Deducing drop size and impact velocity from circular bloodstains," Journal of Forensic Sciences, vol. 50, no. 1, pp. 54-63, 2005.

[2]   M. Lockard, "THE FLUID DYNAMICS OF DROPLET IMPACTS ON INCLINED SURFACES WITH APPLICATION TO FORENSIC BLOOD-SPATTER ANALYSIS," Mechanical Engineering, MS Thesis, Georgia Tech, 2015.

[3]   S. Kim, Y. Ma, P. Agrawal, and D. Attinger, "How important is it to consider target properties and hematocrit in bloodstain pattern analysis?," Forensic Science International, vol. 266, pp. 178-184, 2016.

[4]   P. Agrawal, L. Barnet, and D. Attinger, "Bloodstains on woven fabric: Simulations and experiments for quantifying the uncertainty on the impact and directional angles," Forensic Science International, vol. 278, pp. 240-252, 2017/09/01/ 2017.

[5]   P. M. Comiskey, A. L. Yarin, and D. Attinger, "Hydrodynamics of back spatter by blunt bullet gunshot with a link to bloodstain pattern analysis," Physical Review Fluids, vol. 2, no. 7, p. 073906, 2017.

[6]   P. M. Comiskey, A. L. Yarin, and D. Attinger, "Theoretical and experimental investigation of forward spatter of blood from a gunshot," Physical Review Fluids, vol. 3, no. 6, p. 063901, Jun 2018, Art. no. 063901.

[7]   D. Attinger, Y. Liu, T. Bybee, and K. De Brabanter, "A data set of bloodstain patterns for teaching and research in bloodstain pattern analysis: Impact beating spatters," Data in Brief, vol. 18, pp. 648-654, 2018.

[8]   D. Attinger, Y. Liu, R. Faflak, Y. Rao, B. A. Struttman, K. De Brabanter, P. M. Comiskey, and A. L. Yarin, "A data set of bloodstain patterns for teaching and research in bloodstain pattern analysis: gunshot backspatters," vol. 22, pp. 269-278, 2019.

[9]   T. L. Laber, B. P. Epstein, and M. C. Taylor, "High speed digital video analysis of bloodstain pattern formation from common bloodletting mechanisms," IABPA News, pp. 4-12, 2008.

[10]   P. M. Comiskey, A. L. Yarin, and D. Attinger, "High-Speed Video Analysis of Forward and Backward Spattered Blood Droplets," Forensic Science International, vol. 276, pp. 134-141, 2017.

[11]   R. M. Arthur, P. J. Humburg, J. Hoogenboom, M. Baiker, M. C. Taylor, and K. G. de Bruin, "An image-processing methodology for extracting bloodstain pattern features," Forensic Science International, vol. 277, pp. 122-132, 2017/08/01/ 2017.

[12]   T. C. de Castro, M. C. Taylor, D. J. Carr, J. Athens, and J. A. Kieser, "Storage life of whole porcine blood used for bloodstain pattern analysis," Canadian Society of Forensic Science Journal, vol. 49, no. 1, pp. 26-37, 2016/01/02 2016.

[13]   A. Kolbasov, P. Comiskey, R. P. Sahu, S. Sinha-Ray, A. L. Yarin, B. S. Sikarwar, S. Kim, T. Z. Jubery, and D. Attinger, "Blood Rheology in Shear and Uniaxial Elongation," Rheologica Acta, vol. 55, pp. 901-908, 2016.

[14]   N. Kabaliuk, M. C. Jermy, E. Williams, T. L. Laber, and M. C. Taylor, "Experimental validation of a numerical model for predicting the trajectory of blood drops in typical crime scene conditions, including droplet deformation and breakup, with a study of the effect of indoor air currents and wind on typical spatter drop trajectories," Forensic Sci Int, vol. 245, pp. 107-20, Dec 2014.

[15]   N. Laan, K. G. de Bruin, D. Slenter, J. Wilhelm, M. Jermy, and D. Bonn, "Bloodstain Pattern Analysis: implementation of a fluid dynamic model for position determination of victims," Sci Rep, Article vol. 5, p. 11461, 2015.

[16]   D. Attinger, C. Moore, A. Donaldson, A. Jafari, and H. A. Stone, "Fluid dynamics topics in bloodstain pattern analysis: comparative review and research opportunities," (in eng), Forensic Sci Int, vol. 231, no. 1-3, pp. 375-96, 2013.

[17]   C. Bresteau, S. Guigui, P. Berthier, J. M. Fernandez, and Ieee, "ON THE SECURITY OF AERONAUTICAL DATALINK COMMUNICATIONS: PROBLEMS AND SOLUTIONS," in

2018 Integrated Communications, Navigation, Surveillance Conference(Integrated Communications Navigation and Surveillance Conference, New York: Ieee, 2018.

[18]   M. Grabmuller, P. Cachee, B. Madea, and C. Courts, "How far does it get?--The effect of shooting distance and type of firearm on the simultaneous analysis of DNA and RNA from backspatter recovered from inside and outside surfaces of firearms," (in Eng), Forensic Sci Int, Research Support, Non-U.S. Gov't vol. 258, pp. 11-8, Jan 2016.

[19]   C. Rossi, L. D. Herold, T. Bevel, L. McCauley, and S. Guadarrama, "Cranial Backspatter Pattern Production Utilizing Human Cadavers," J Forensic Sci, vol. 63, no. 5, pp. 1526-1532, Sep 2018.

[20]   B. G. Stephens and T. B. Allen, "Back spatter of blood from gunshot wounds. Observations and experimental simulation," Journal of Forensic Sciences, vol. 28, no. 2, pp. 437-439, 1983.

[21]   S. Siu, J. Pender, F. Springer, F. Tulleners, and W. Ristenpart, "Quantitative Differentiation of Bloodstain Patterns Resulting from Gunshot and Blunt Force Impacts," (in eng), J Forensic Sci, pp. 1-14, Feb 10 2017.

[22]   P. M. Comiskey, A. L. Yarin, S. Kim, and D. Attinger, "Prediction of blood back spatter from a gunshot in bloodstain pattern analysis," Physical Review Fluids, vol. 1, no. 4, p. 043201, 2016.

[23]   Anonymous, "literature search for the distance that backspatter travels," IABPA News, vol. 23, no. 3, September 2017, pp. 31-32, 2007.

[24]   S. H. James, P. E. Kish, and T. P. Sutton, Principles of Bloodstain Pattern Analysis: Theory and Practice. CRC Press, 2005.

[25]   H. L. MacDonell, Bloodstain Patterns, 2nd. ed. Laboratory of Forensic Sciences, Corning, NY USA, 2005.

[26]   P. R. D. Forest, R. E. Gaensslen, and H. C. Lee, Forensic science: An introduction to criminalistics. McGraw-Hill, New York, 1983.

[27]   J. O. Pex and C. H. Vaughan, "Observations of high velocity bloodspatter on adjacent objects," Journal of Forensic Sciences, vol. 32, no. 6, pp. 1587-1594, 1987.

[28]   B. Karger, R. Nüsse, B. Brinkmann, G. Schroeder, and S. Wüstenbecker, "Backspatter from experimental close-range shots to the head: 1. Macrobackspatter," (in English), International journal of legal medicine, vol. 109, no. 2, pp. 66-74, 1996/10/01 1996.

[29]   B. Karger, R. Nüsse, H. D. Tröger, and B. Brinkmann, "Backspatter from experimental close-range shots to the head: 2. Microbackspatter and the morphology of bloodstains," Int J Legal Med (1997) 110 : 27-30, 1997.

[30]   T. Bevel and R. M. Gardner, 2, Ed. Bloodstain Pattern Analysis with an Introduction to Crime Scene Reconstruction. CRC Press, Boca Raton, FL, USA, 2002.

[31]   J. Bockrath and R. Lugo, "Slugger Slaying Caught on Tape," in 2017 Annual IABPA Training Conference (International Association of Bloodstain Pattern Analysts), Crown Plaza Redondo Beach and Marina, 2017.

[32]   F. Camana, "Determining the area of convergence in Bloodstain Pattern Analysis: A probabilistic approach," Forensic Science International, vol. 231, no. 1-3, pp. 131-136, Sep 10 2013.

[33]   D. Attinger, P. Comiskey, A. Yarin, and K. De Brabanter, "Determining the region of origin of blood spatters considering fluid dynamics and statistical uncertainties," being finalized for Forensic Science International (status January 2018).

[34]   T. G. Theofanous, "Aerobreakup of Newtonian and Viscoelastic Liquids," Annual Review of Fluid Mechanics, vol. 43, no. 1, pp. 661-690, 2011.

[35]   G. M. Faeth, L. P. Hsiang, and P. K. Wu, "Structure and breakup properties of sprays," International Journal of Multiphase Flow, vol. 21, pp. 99-127, Dec 1995.

[36]   M. Vargas, "Drag Coefficient of Water Droplets Approaching the Leading Edge of an Airfoil," 5th AIAA Atmospheric and Space Environments Conference, pp. 1-23, DOI:10.2514/6.2013-3054, 2013.

[37]   E. Loth, "Quasi-steady shape and drag of deformable bubbles and drops," (in English), International Journal of Multiphase Flow, Review vol. 34, no. 6, pp. 523-546, Jun 2008.

[38]   A. Reinhart, "Das Verhalten fallender Tropfen," Chem. Ing. Tech., p. 36, 1964.

[39]   R. Clift, J. R. Grace, and M. E. Weber, Bubbles, drops and particles. New York: Academic, 1978.
[40]   C. D. Adam, "Fundamental studies of bloodstain formation and characteristics," (in Eng), Forensic Sci Int, no. 219, pp. 76-87, 2012.
[41]   R. P. Sahu, S. Sett, A. L. Yarin, and B. Pourdeyhimi, "Impact of aqueous suspension drops onto non-wettable porous membranes: Hydrodynamic focusing and penetration of nanoparticles," Colloids and Surfaces A: Physicochemical and Engineering Aspects, vol. 467, pp. 31-45, 2015.
[42]   B. L. Scheller and D. W. Bousfield, "Newtonian drop impact with a solid surface," AICHE Journal, vol. 41, no. 6, pp. 1357-1367, 1995.
[43]   L. P. Hsiang and G. M. Faeth, "NEAR-LIMIT DROP DEFORMATION AND SECONDARY BREAKUP," International Journal of Multiphase Flow, vol. 18, no. 5, pp. 635-652, Sep 1992.
[44]   G. Recktenwald, Numerical methods with Matlab: Implementations and applications. Upper-Saddle River, NJ.: Prentice-Hall, 2000.
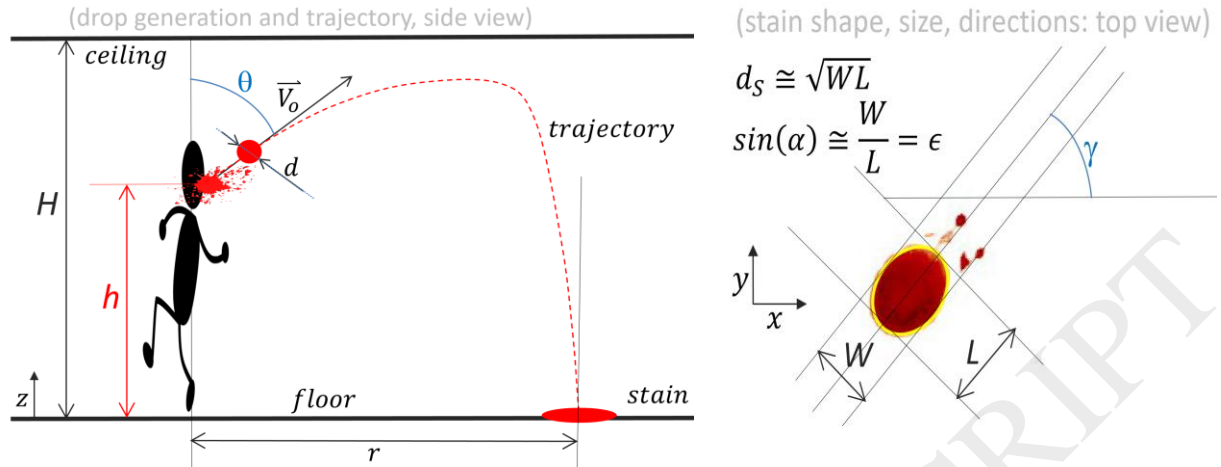
Figure 1: representation of the problem at hand: 'How far can a blood drop travel from a blood source?". The side view describes the controlling variables of the forward problems: two heights (origin and ceiling), the initial velocity V_0 and launch angle θ, as well as the drop diameter d. The top view shows how the main direction of the stain determines the directional angle γ, and how the width W and length L of an ellipse fitted on the stain are used to determine impact angle α and equivalent diameter d_S. We use equivalent diameter because it is simpler to use than stain area for the analyst. In the case of a round stain, the equivalent diameter is simply the diameter of the stain.
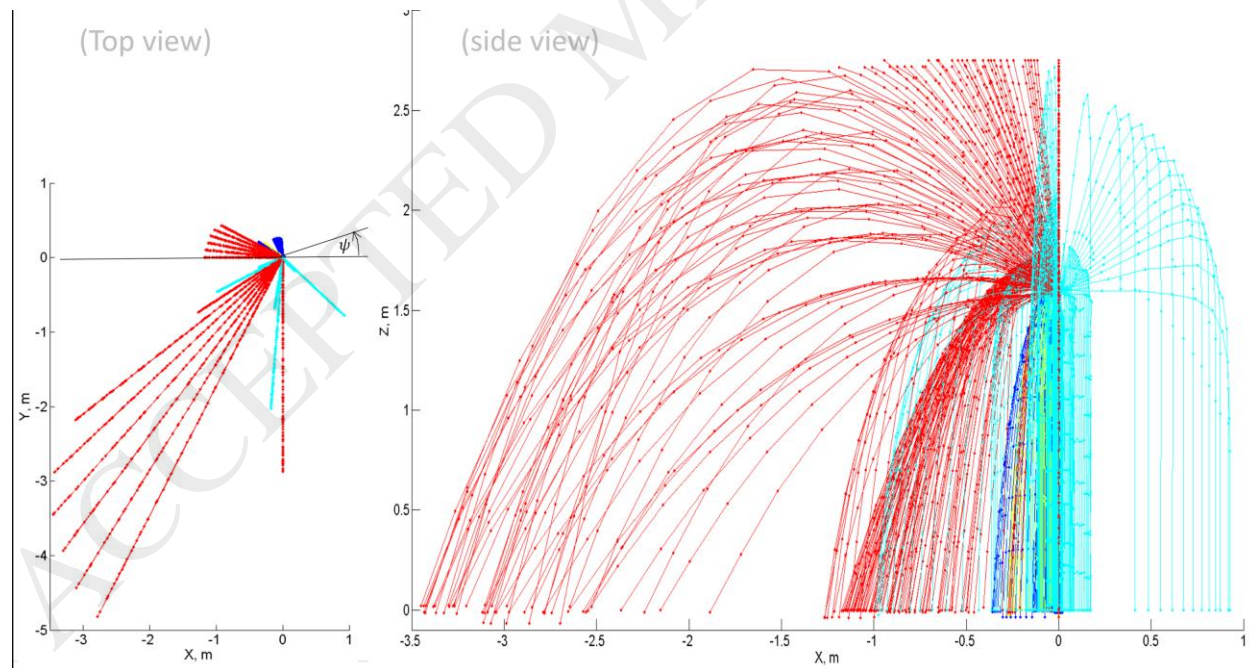
Figure 2: 3D geometry of 2160 simulated trajectories, corresponding to less than 0.5 ‰ of all the simulations performed. Colors inform on the initial and boundary conditions, which are those of the bolded parameters in Table 1. Red means large (d>1mm) and fast (V_0>1m/s) drops; blue, large and slow; cyan small and fast; yellow small and slow. Yellow trajectories are barely visible because small and slow

14

drops do not travel further than a few cm. While all the simulations are calculated in the two-dimensional plane X-Z, the trajectories are plotted with an arbitrary rotation around the vertical axis, set by angle $\psi \in [0,360°]$, to reduce overlap.
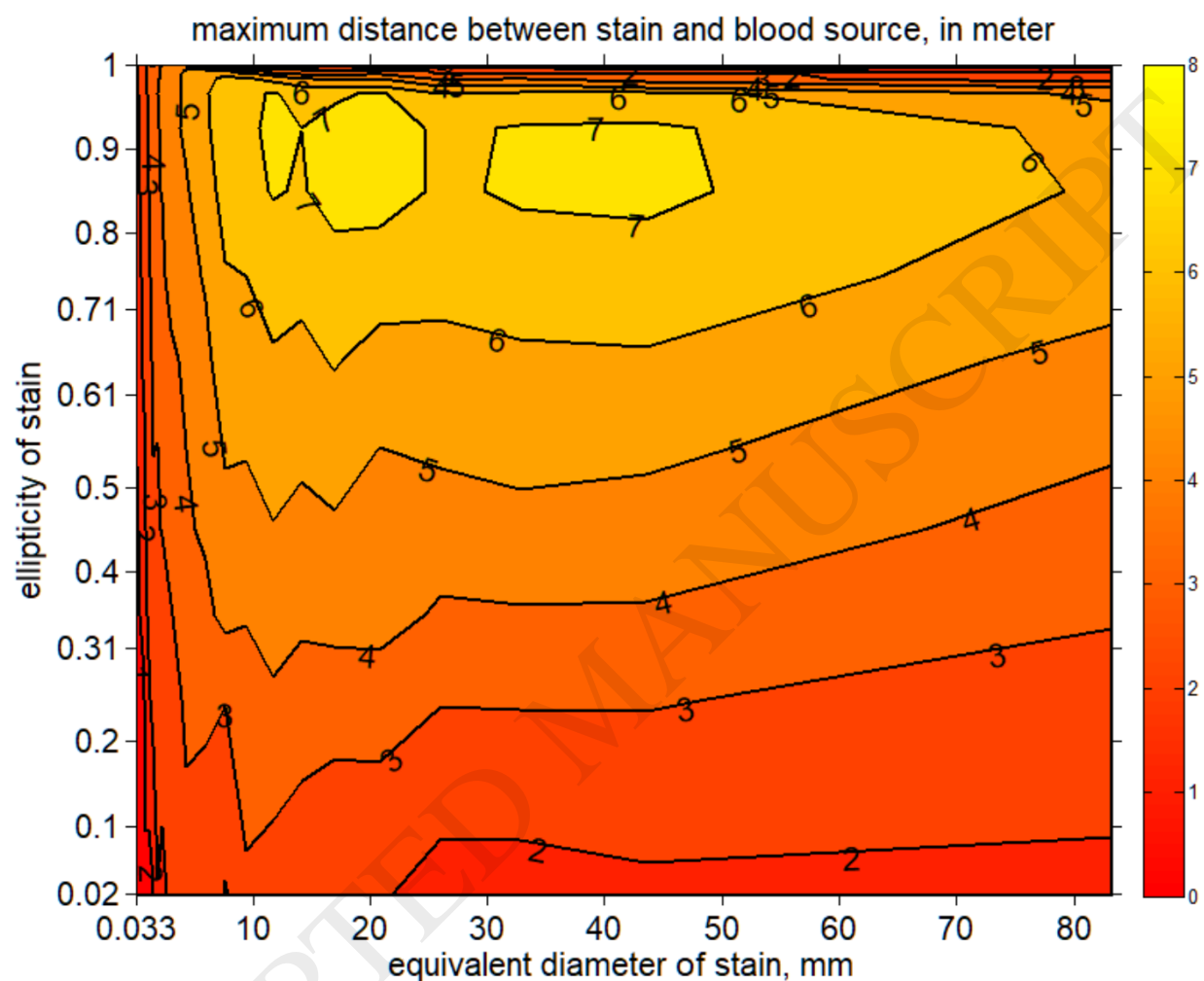

Figure 3: Maximum horizontal distance, in meter, between a stain on the floor of a crime scene and its blood source, as a function of the stain size and shape. Data is generated assuming that the height of the blood source, of the ceiling, the initial velocity and the launch angle, can take any combination of values listed in Table 1.
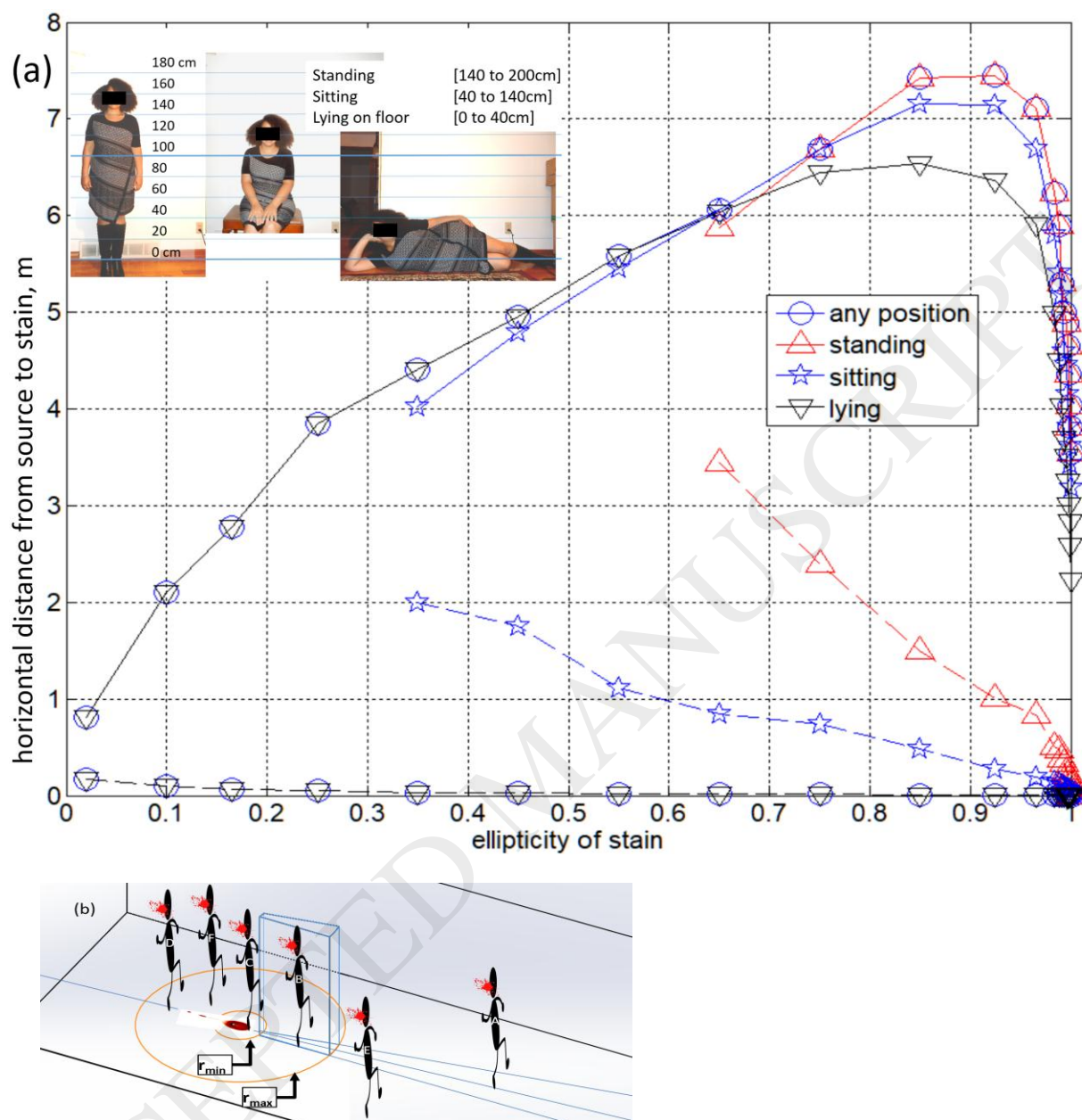
Figure 4: (a) distance in meter between a stain and its blood source as a function of the drop ellipticity and the position of the victim. Minimum distance is hatched, and maximum distance is continuous. Here the positions (standing, sitting or lying on the floor) are described in an exclusive manner in terms of the associated heights. Data generated assuming that the height of the ceiling, and the initial velocity, drop size and the launch angle, can take any combination of values listed in Table 1. Example (b) of using chart in Figure 4a. Based on a measurement of stain ellipticity, Figure 4a provides the minimum and maximum distance between stain and source, which are respectively labelled r_{min} and r_{max}. Together with the direction of the main axis of the stain (indicated in blue with its uncertainty), the possible location of the blood source is identified as a wedge-like "piece of cake" with blue edges. In Figure 4b, multiple possible source positions are labeled A-F, and only position B is compatible with the shape and orientation of the represented stain.
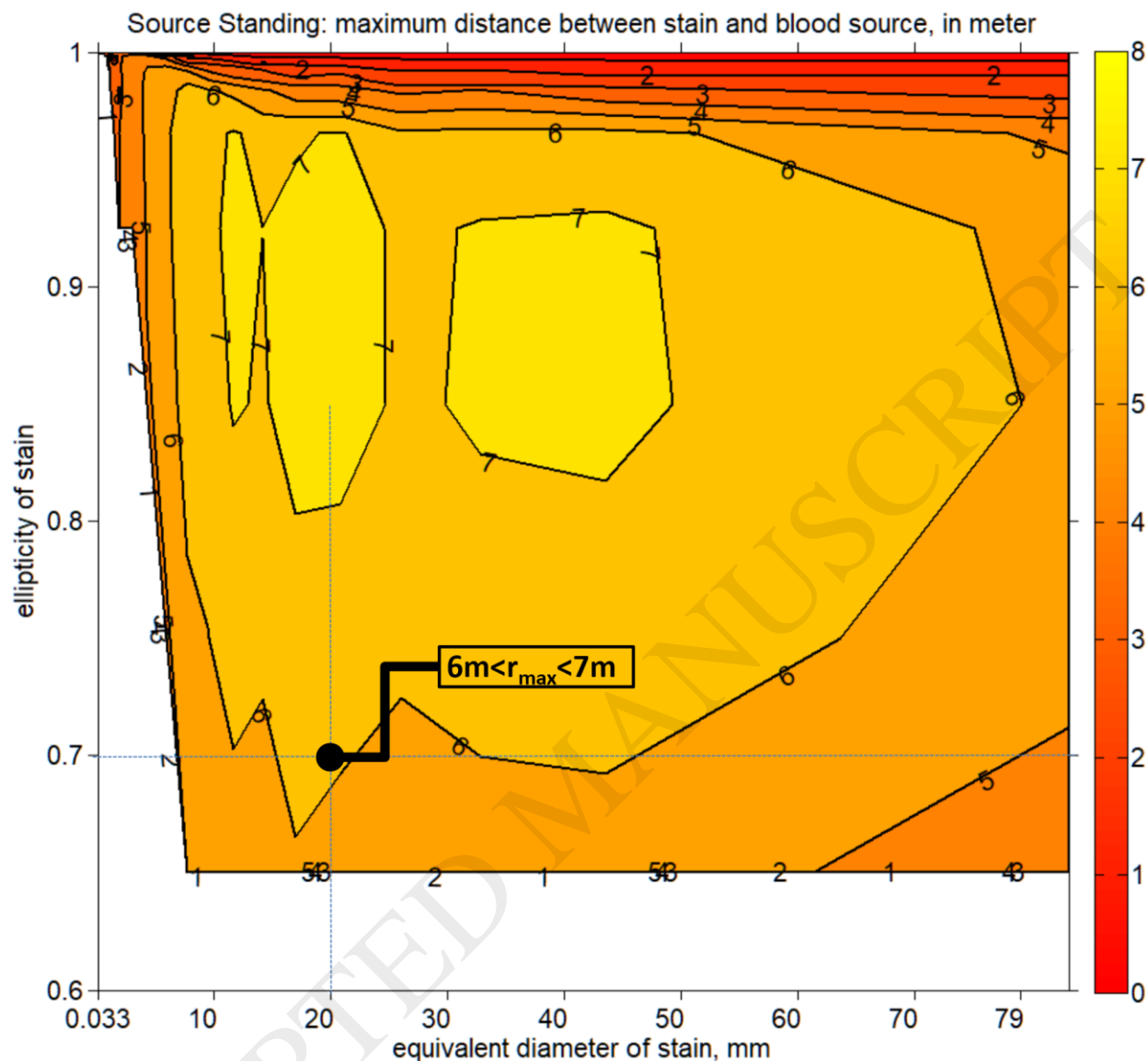
Figure 5: Maximum horizontal distance, in meter, between a stain and its blood source, as a function of the drop size and velocity. Source height is between 140cm and 200cm. Ceiling height, drop size, launch angle and drop velocity can take any value in Table 1. Result indicated by the bold connector corresponds to the maximum radius in Figure 4b.
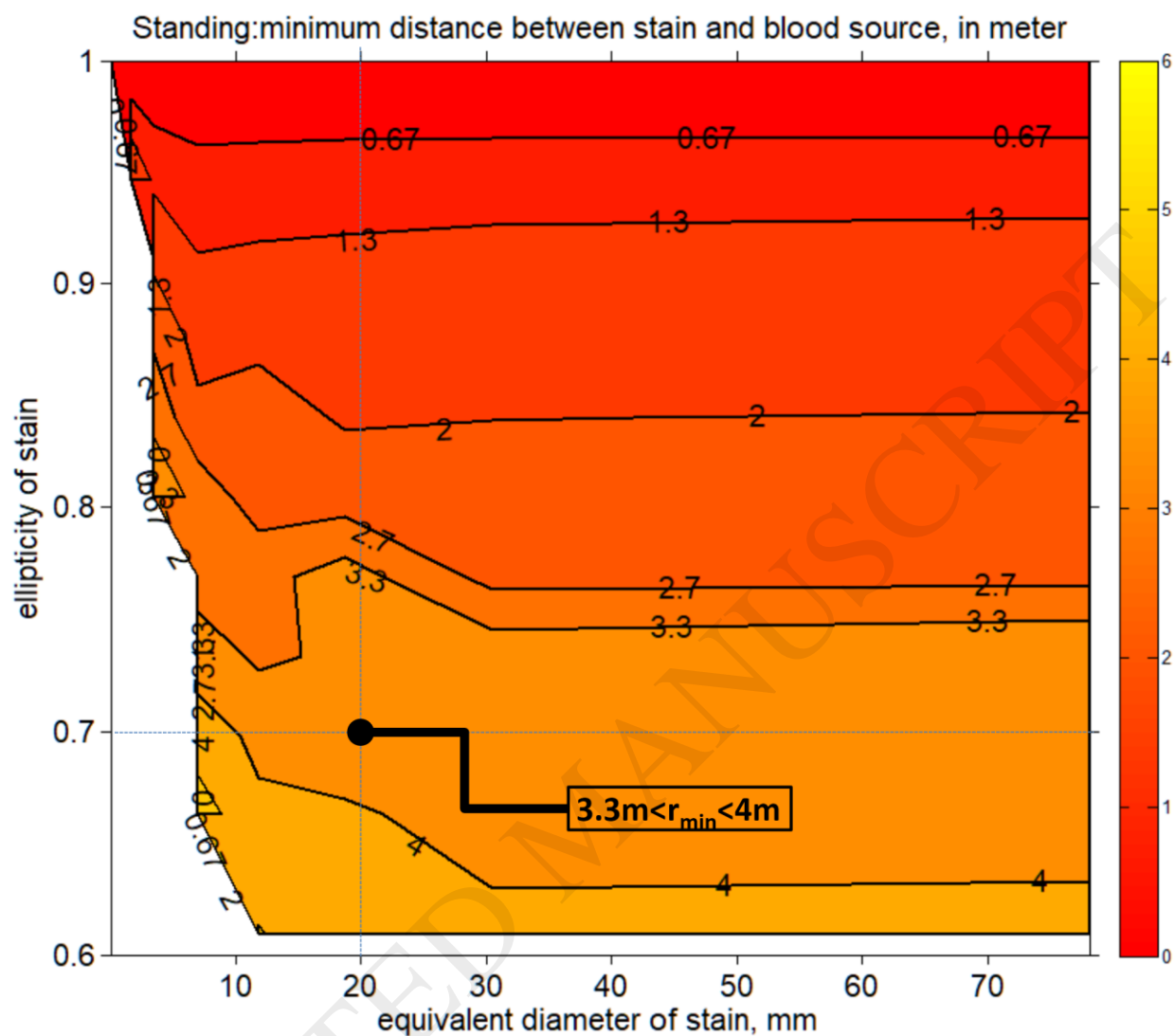
Figure 6: Minimum horizontal distance, in meter, between a stain and its blood source, as a function of the drop size and velocity. Source height is between 140cm and 200cm. Ceiling height, drop size, launch angle and drop velocity can take any value in Table 1. Result indicated by the bold connector corresponds to the minimum radius r_{min} in Figure 4b.
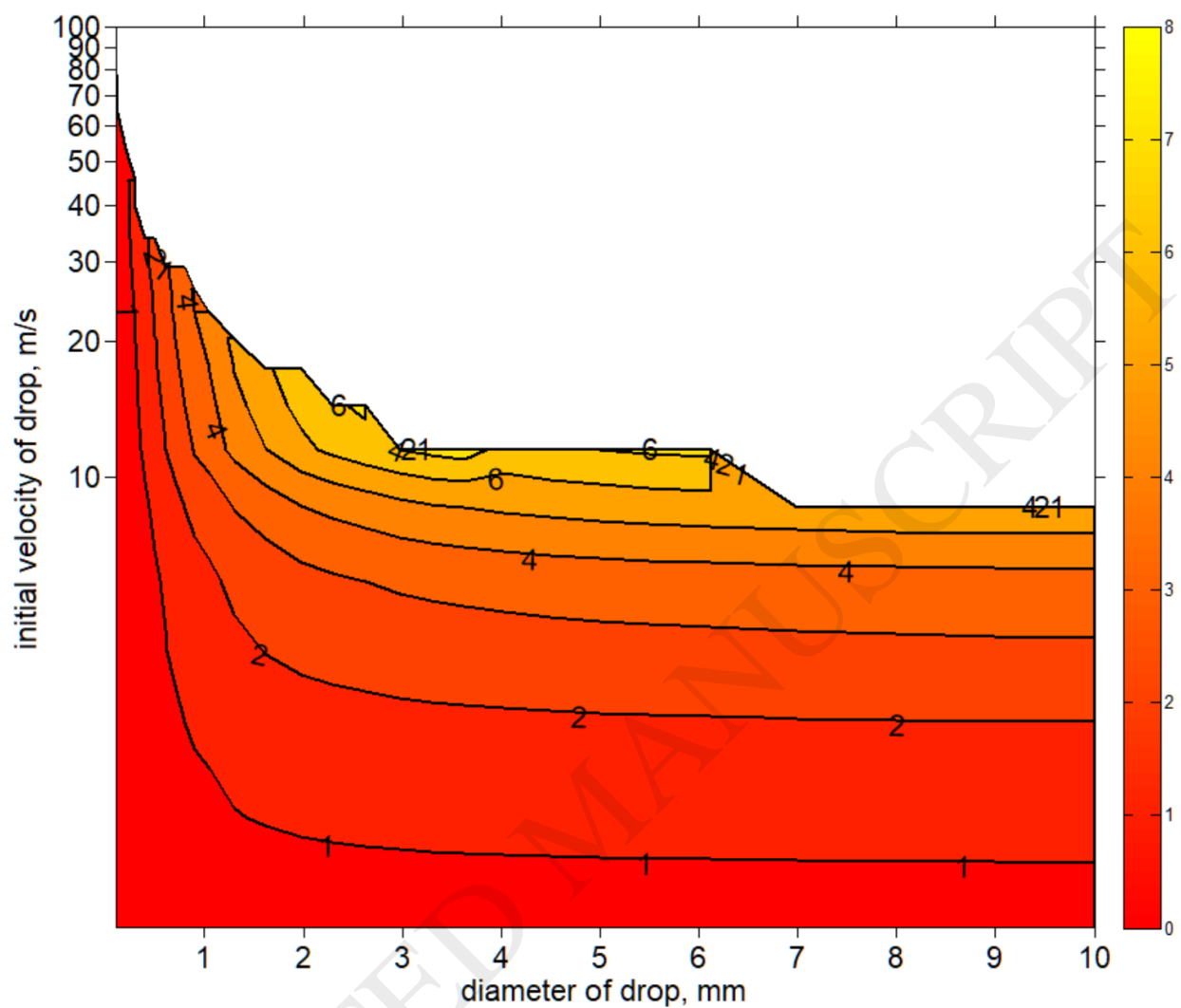
Figure 7: The colors represent the horizontal distance between a stain and a blood source, as a function of the initial velocity of the drop and the diameter of the drop. Regions without color correspond to breakup in flight. Data generated assuming that the height of the blood source, of the ceiling, and launch angle can take any combination of values listed in Table 1.
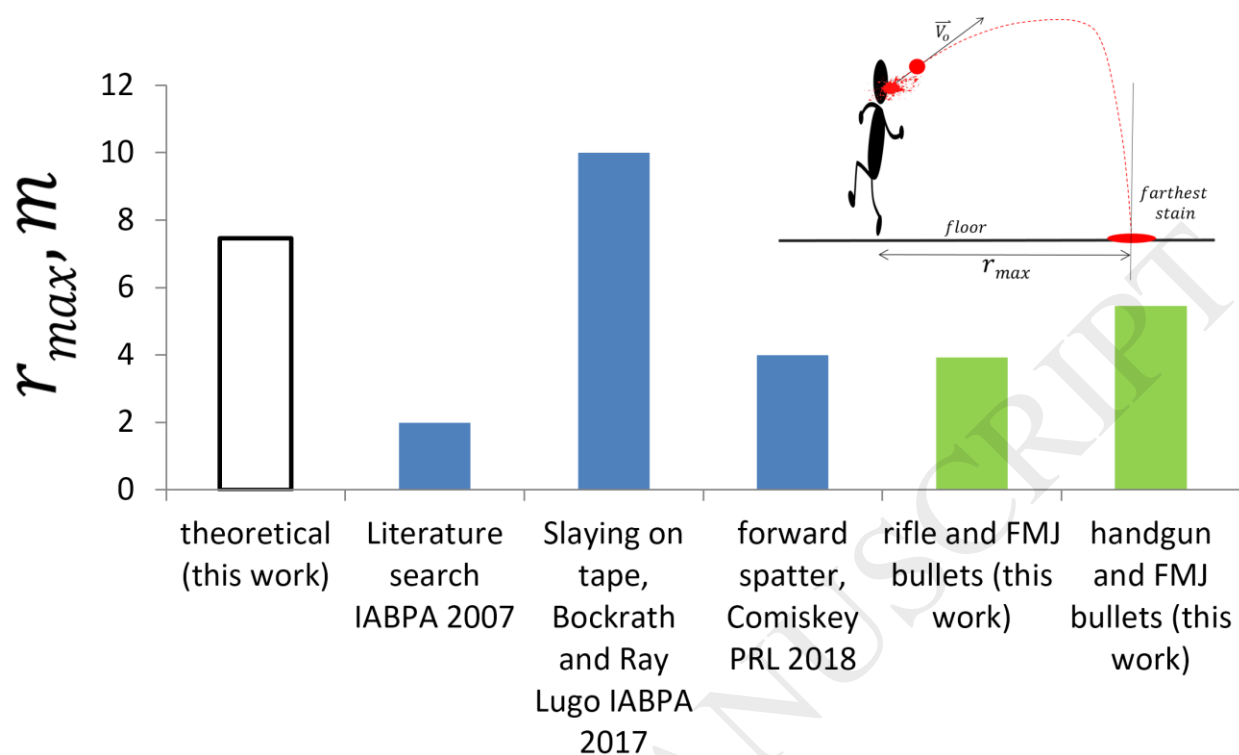
Figure 8: Reported maximum horizontal distance between stains and blood source, r_{max}. Comparison of simulations in this work and various experiments in the published literature [6, 23, 31] and performed for this study.

Parameter, symbol, unit	Number of values	[minimum, increment, maximum – separated by commas] or [list of values separated by space]
Ceiling height, H, m	9 (**1**)	[2.5 **2.75** 3 3.25 3.5 3.75 4 4.25 4.5]
Blood source height, h, m	21 (**1**)	[0 10 20 30 40 50 60 70 80 90 100 110 120 130 140 150 **160** 170 180 190 200]
Launch angle θ, degree	28 (**15**)	[**0** 5 **10** 15 **20** **25** 27.5 **30** 32.5 **35** 37.5 **40** 42.5 **45** 47.5 **50** 52.5 **55** 57.5 **60** 62.5 **65** 67.5 **70** 75 **80** 85 **90**]
Drop diameter d, mm	29 (**12**)	[**0.033 0.066 0.1** 0.2 **0.3** 0.4 0.5 0.6 **0.7** 0.8 0.9 **1** 1.3. 1.6 **2** 2.3 2.6 **3** 3.3 3.6 **4** 4.5 **5** 5.5 6 **7** 8 9 **10**]
Initial velocity V_0, m/s	35 (**12**)	[**0.01** 0.015 0.02 0.03 0.04 **0.05** 0.075 **0.1** 0.25 **0.5** 0.75 **1 2** 3 **4** 5 **7.5 10** 12.5 15 17.5 **20** 22.5 25 27.5 **30** 35 40 45 50 60 70 80 90 **100**]

Table 1: list of the discrete parameters used in the trajectory simulations. Total number of simulations considered in this manuscript is the product of each number of values: 5.63 million of simulations. A smaller set of parameters, in bold, is plotted in the example Figure 2.

Gun label	description
Rock River Arms rifle .223''	LAR-15 16'' barrel length M-4, .223 caliber (5.66 mm), with Yankee Hill YHM Phantom 223 suppressor
S&W 9 mm	Smith and Wesson M&P Caliber 9mm, with 4.25'' barrel length.

Bullet label (tip shape)	Velocity, m/s	Full description	Picture
AE223 (pointy)	~987	FMJ rifle rounds, Federal Ammunition American Eagle #AE223, bullet mass 55 grain, .223 rem.	
AE9FP (flat)	285	FMJ flat nose handgun ammunition, Federal Ammunition American Eagle #AE9FP, 147 grain, 9 mm.	

Table 2: guns and bullets used in the experiments, with #manufacturer number. Velocities are either as per manufacturer data (and preceded with the symbol "~") or measured with a chronograph at the shooting range. The grain is a measure of mass, and can be converted to SI units as 1 grain $\cong$ 64.8 mg. Pictured ruler has cm units.

21